Global Ecology and Conservation 24 (2020) e01393

Contents lists available at ScienceDirect

Global Ecology and Conservation

journal homepage: http://www.elsevier.com/locate/gecco

Original Research Article

Predicting bycatch hotspots in tropical tuna purse seine fisheries at the basin scale

Laura Mannocci*, Fabien Forget, Mariana Travassos Tolotti, Pascal Bach, Nicolas Bez, Hervé Demarcq, David Kaplan, Philippe Sabarros, Monique Simier, Manuela Capello, Laurent Dagorn

MARBEC, Univ Montpellier, CNRS, Ifremer, IRD, Sète, France

ARTICLE INFO

Article history:
Received 12 August 2020
Received in revised form 27 November 2020
Accepted 27 November 2020

Keywords:
Bycatch
Habitat modelling
Hotspots
Fisheries observer programs
Geographical extrapolation
Tropical oceans

ABSTRACT

Fisheries observer programs represent the most reliable way to collect data on fisheries bycatch. However, their limited coverage leads to important data gaps that preclude bycatch mitigation at the basin scale. Habitat models developed from available fisheries observer programs offer a potential solution to fill these gaps. We focus on tropical tuna purse seine fisheries (TTPSF) that span across the tropics and extensively rely on floating objects (FOBs) for catching tuna schools, leading to the bycatch of other species associated with these objects. Bycatch under floating objects is dominated by five species, including the vulnerable silky shark *Carcharhinus falciformis* and four bony fishes (oceanic triggerfish *Canthidermis maculata*, rainbow runner *Elagatis bipinnulata*, wahoo *Acanthocybium solandri*, and dolphinfish *Coryphaena hippurus*). Our objective was to predict possible bycatch hotspots associated with FOBs for these five species across two tropical oceans. We used bycatch data collected from observer programs onboard purse seiners in the Atlantic and Indian oceans. We developed a generalized additive model per species and per ocean relating bycatch to a set of environmental covariates (depth, chlorophyll-a concentration, sea surface temperature, mixed layer depth, surface salinity, total kinetic energy and the density of floating objects) and temporal covariates (year and month). We extrapolated modeled relationships across each ocean within the range of environmental covariates associated with the bycatch data and derived quarterly predictions. We then detected bycatch hotspots as the 90th percentiles of predictions. In the Atlantic Ocean, bycatch hotspots were predicted throughout tropical and subtropical waters with little overlap between species. By contrast in the Indian Ocean, major overlapping hotspots were predicted in the Arabian Sea throughout most of the year for four species, including the silky shark. Our modeling approach provides a new analytical way to fill data gaps in fisheries bycatch. Even with the lack of evaluation inherent to extrapolations, our modeling effort represents the first step to assist bycatch mitigation in TTPSF and is applicable beyond these fisheries.

* Corresponding author. Avenue Jean Monnet CS 30171, 34203, Sète cedex, Sète, France.
E-mail address: laura.mannocci@ird.fr (L. Mannocci).

https://doi.org/10.1016/j.gecco.2020.e01393

1. Introduction

Bycatch, i.e., the incidental capture of non-target species by fisheries, is a major threat to pelagic ecosystems (Ortuño Crespo and Dunn, 2017). Bycatch raises conservation concerns for long-lived, late maturing species that are particularly sensitive to anthropogenic impacts (Lewison et al., 2014). Through the selective removal of species, bycatch may also alter the structure and functioning of pelagic ecosystems (Kitchell et al., 2002). Fisheries observer programs represent the most reliable and accurate way to collect data on bycatch (Roda et al., 2019). In the framework of these programs, scientific observers embark on fishing vessels to quantify species-specific bycatch associated with fishing operations. However, the high financial and logistical costs induced by these programs preclude their widespread implementation. Gilman et al. (2014) estimated that two thirds of fisheries managed by regional fisheries management organizations (RFMOs) lack adequate observer coverage. Although observer coverage has increased since this estimate was made, observer coverage remains undeniably heterogeneous across regions, leading to sparse bycatch data at the scale of ocean basins.

Fisheries observer programs also provide crucial information on the distribution of poorly known fish and shark species that can be used to develop habitat models (Lezama-Ochoa et al., 2016; Lopez et al., 2020; Scales et al., 2017). Habitat models (HMs), also called species distribution models or ecological niche models, are powerful statistical tools for predicting species occurrences and abundances in areas of sparse data (Elith and Leathwick, 2009). Using these models, species-habitat relationships estimated from available species observations and environmental data may be carefully predicted at the scale of ocean basins within the range of environmental conditions associated with the data (Mannocci et al., 2015; Redfern et al., 2017; Virgili et al., 2019). In this study, we combined HMs and available fisheries observer programs to predict hotspots of bycatch in tropical tuna purse seine fisheries at the scale of two oceans.

Tropical tuna purse seine fisheries (TTPSF) catch close to 5 million tons of tuna per year across fishing grounds in the three tropical oceans, representing two thirds of the global tuna catch (ISSF, 2019). Large multispecies aggregations occur at floating objects in the world's tropical oceans and are used by TTPSF to target tropical tunas. These floating objects include natural objects (such as logs) and man-made drifting fish aggregating devices (DFADs) that are massively deployed by fishers (Dagorn et al., 2013a). As such, fishing on floating objects leads to up to 5 times more bycatch per tuna ton than fishing on free-swimming tuna schools (Amandè et al., 2010; Kaplan et al., 2014). Though bycatch in TTPSF is significantly lower than in some other fisheries (with reported discards rates of 3.9% in TTPSF *versus* 12.3% in pelagic longlines fisheries for example) (Roda et al., 2019), the sheer magnitude of TTPSF means that the amount of fishing-induced mortality is significant.

Bycatch under floating objects is dominated by few species, including the silky shark and four bony fishes (oceanic triggerfish, rainbow runner, wahoo, and dolphinfish) (Dagorn et al., 2013b). Silky sharks are particularly vulnerable to overexploitation due to their slow growth, late maturation and low fecundity (Cortés et al., 2010). The bony fishes are less sensitive to overexploitation, but form an important community whose removal may alter the pelagic ecosystem's balance (Dagorn et al., 2013b). Characterizing species-specific bycatch hotspots at the basin scale is of extreme importance given the high levels of fishing pressure and extensive distribution of TTPSF.

In this study, our objective was to predict bycatch hotspots associated with floating objects for these five species at the scale of two tropical oceans. We developed HMs to relate species-specific bycatch under floating objects derived from observer programs onboard purse seiners in the tropical Atlantic and Indian Oceans to a suite of environmental and temporal covariates. We then used the modeled relationships to derive predictions of potential bycatch hotspots across each tropical ocean. Our modeling approach offers a solution to fill the current gaps in fisheries observer programs and can help direct bycatch mitigation efforts at the basin scale.

2. Material and methods

2.1. Fisheries observer data

We used data from observer programs collected onboard French tuna purse seiners between 2014 and 2018 in the tropical Atlantic Ocean (AO) and the western Indian Ocean (IO). Observer data were collected through the European Union Data Collection Framework (DCF, EU regulation 199/2008), the Moratoria program of the International Commission for the Conservation of Atlantic Tunas (ICCAT), and the OCUP program (*Observateur Commun Unique et Permanent*) of the French producer organization ORTHONGEL (Cauquil et al., 2015). During this period, mean observer coverage rates were 95% in the AO and 42% in the IO.

All three data collection programs followed the same standardized protocol. For each fishing set, dedicated observers recorded the date, time, geographical coordinates, and total estimated bycatch per species in number of individuals whenever possible (or otherwise in weight), along with the estimated mean individual length. When total weight was reported, the number of individuals was derived by dividing the total weight by the mean individual weight inferred from the recorded length after conversion using published length-weight relationships (Cauquil et al., 2015). For this analysis, we only considered observed fishing sets under floating objects (FOBs) because our objective was to predict bycatch associated with FOBs.

Fisheries observer data were available for 4331 FOBs fishing sets (representing 45% of all observed sets) in the AO and for 6154 FOBs fishing sets (representing 73% of all observed sets) in the IO (Fig. A-1). Silky shark (FAO code: FAL), oceanic

triggerfish (CNT), rainbow runner (RRU), wahoo (WAH), and dolphinfish (DOL) were the dominant bycatch species in both oceans (Fig. A-2). Their occurrences ranged from 35% to 69% of FOBs fishing sets in the AO and from 39% to 76% in the IO (Fig. A-3).

2.2. Environmental covariates

We selected a suite of environmental covariates based on their availability and ecological relevance to tropical pelagic fishes (detailed in Table B-1): depth, chlorophyll-a concentration (CHL), sea surface temperature (SST), mixed layer depth (MLD), surface salinity (SAL), total kinetic energy (TKE) and the density of floating objects (FOBs_DENS). The first six covariates were extracted for the 2014–2018 study period from the NOAA National Geophysical Data Center (https://data.nodc.noaa.gov/cgi-bin/iso?id=gov.noaa.ngdc.mgg.dem:316), the Nasa OceanColor website (https://oceancolor.gsfc.nasa.gov/atbd/sst/) and the EU Copernicus marine environment monitoring service (https://marine.copernicus.eu/). Their spatial resolutions ranged from 1/60° to 1/12° and their temporal resolutions from days to months (Table B-1). All six environmental covariates were standardized to strata of 1 ° × 1 ° x month (our desired spatio-temporal resolution for basin-scale predictions) using nearest neighbor resampling in each ocean (Figs. B-1 to B-6).

We also included FOBs_DENS as an environmental covariate in our HMs, processed as follows. All DFADs and some natural objects are equipped with satellite transmitters that provide daily GPS positions (Maufroy et al., 2015). We obtained individual objects positions from satellite transmitters belonging to the French tropical tuna purse seine fishery from 2014 to 2018 and linearly interpolated them at midnight GMT on each day. Interpolated FOBs positions were then assigned to 1 ° × 1 ° grid cells, summed per month, and divided by the number of days in each month to derive FOBs_DENS (Katara et al., 2018). The density of objects positions from the French fleet was considered a reasonable proxy of the overall density of FOBs. Similarly to the other covariates, FOBs_DENS was standardized to strata of 1 ° × 1 ° x month (Fig. B-7).

Finally, values of all seven covariates were assigned to fishing sets based on these 1 ° × 1 ° x month strata (Fig. A-4). Numbers of captured individuals per 1 × 1° x month strata are shown in Figs. A-5 to A-9.

2.3. Habitat modeling

2.3.1. Model fitting and evaluation

We developed generalized additive models (GAMs) (Wood, 2017) per species and per ocean using the numbers of captured individuals per FOB fishing set as the response variable. GAMs are flexible regression techniques that rely on smooth functions for estimating non-linear and non-monotonic relationships between a response and covariates (Wood, 2017). In these models, a link function *g()* relates the mean of the response variable Y given the covariates X_i to an additive predictor as follows:

$$g(E(Y|X_i)) = \alpha + \sum f_i(X_i)$$

where f_i is a smoothing function of the covariate X_i and α is the intercept. Covariates included the seven above environmental covariates, as well as two purely temporal covariates (month and year) to account for seasonal and inter-annual variability in species abundance and observed fishing effort (e.g., Gilman et al., 2012). Spearman's rank correlation coefficients between environmental covariates ranged from 0.01 to 0.56 and from 0.02 to 0.53 in absolute value in the Atlantic and Indian oceans, respectively (Figs. B-8 and B-9), indicating little collinearity. They could thus be included in the same model without leading to instability in parameter estimation (Zuur et al., 2010). Environmental covariates were modeled with thin-plate regression splines smoothers with shrinkage to allow non-significant terms to be removed from the model during fitting (Wood and Augustin, 2002). The basis dimension of smoothers was restricted to 5 to control for overfitting (e.g., Fisher et al., 2018). Year and month were modeled with thin-plate and cubic regression spline smoothers, respectively. In addition to these fixed effect smoothers, random effect smoothers of observers and vessels were included to account for observer- and vessel-specific heterogeneities in the data. All smooth terms were optimized using the restricted maximum likelihood criterion that penalizes overfitting and leads to more pronounced optima (Wood, 2011).

Regression-based tests of the null hypothesis of equi-dispersion (i.e., Poisson GAMs) against the alternative of over-dispersion (Cameron and Trivedi, 1990) (implemented in the 'AER' package (Kleiber and Zeileis, 2019)) indicated over-dispersion for all species in both oceans. Therefore, we considered both negative binomial and tweedie distributions (with log link function) that are well suited to model over-dispersed count data (Candy, 2009; Richards, 2008). For each species and ocean, we ranked negative binomial and tweedie GAMs based on Akaike's information criterion scores. We then used a backward stepwise procedure for variable selection, considering a p-value of 0.01 as the threshold for exclusion of non-significant covariates.

Model goodness of fit was evaluated by calculating the percentage of mean absolute error (PMAE), i.e., the mean absolute error divided by the mean abundance (a PMAE > 100% would indicate an average error higher than the average abundance and thus a poor fit). Diagnostic plots of residuals were examined, including quantile-quantile plots of deviance residuals (Augustin et al., 2012) and plots of randomized quantile residuals (Dunn and Smyth, 1996) *versus* the linear predictor.

Table 1
Summary of selected models across species and oceans. P-values are reported for all covariates and random-effects (NS correspond to non-significant covariates with a p-value > 0.01 dropped from the models). DE: deviance explained indicating model explanatory power. PMAE: percentage mean absolute error indicating goodness of fit (indicative values: PMAE > 100%: poor; PMAE ∈ [50%–100%]: fair to good; PMAE < 50%: excellent). Environmental covariates: CHL: chlorophyll concentration; SST: sea surface temperature; SAL: surface salinity, MLD: mixed layer depth; TKE: total kinetic energy; FOBs_DENS: floating objects density. Statistical distributions (Stat. distrib.): Nb: negative binomial, Tw: tweedie.

Species	Ocean	Stat. distri.	Environmental covariates							Temporal covariates		Random effects		Dev. Expl. (%)	PMAE (%)
			DEPTH	SST	CHL	MLD	TKE	SAL	FOBs_DENS	Year	Month	Observer	Vessel		
Silky shark (FAL)	Atlantic	Nb	< 0.001	< 0.001	< 0.001	< 0.001	NS	NS	< 0.001	< 0.001	< 0.001	< 0.001	< 0.001	20.1	74.7
	Indian	Nb	< 0.005	NS	NS	< 0.005	NS	< 0.001	NS	< 0.001	< 0.001	< 0.001	< 0.001	12.7	52.8
Oceanic triggerfish (CNT)	Atlantic	Tw	< 0.001	< 0.001	< 0.001	< 0.001	NS	< 0.001	< 0.001	< 0.001	< 0.001	< 0.001	< 0.001	25.0	70.3
	Indian	Tw	< 0.005	< 0.001	NS	< 0.005	< 0.005	NS	NS	< 0.001	< 0.001	< 0.001	< 0.005	20.4	77.2
Rainbow runner (RRU)	Atlantic	Tw	< 0.001	< 0.001	NS	< 0.001	< 0.005	NS	< 0.001	< 0.001	< 0.001	< 0.001	< 0.001	29.4	80.2
	Indian	Tw	< 0.005	NS	< 0.001	NS	NS	< 0.001	NS	< 0.001	< 0.001	< 0.001	NS	19.1	68.9
Wahoo (WAH)	Atlantic	Nb	< 0.001	< 0.001	< 0.001	< 0.001	NS	< 0.005	< 0.001	< 0.005	< 0.001	< 0.001	< 0.005	26.9	75.6
	Indian	Nb	< 0.001	< 0.001	NS	NS	NS	< 0.001	NS	NS	< 0.001	< 0.001	NS	16.7	71.4
Dolphinfish (DOL)	Atlantic	Nb	< 0.001	< 0.001	NS	NS	NS	< 0.001	NS	< 0.001	< 0.001	< 0.001	NS	22.5	71.2
	Indian	Tw	NS	< 0.001	NS	< 0.001	NS	< 0.001	NS	< 0.005	< 0.001	< 0.001	< 0.005	17.5	64.9

GAMs were developed using the 'mgcv' package (Wood, 2019) in R.

2.3.2. Predictions of bycatch at the basin scale

For each species and ocean, the best selected model was used to predict bycatch (in number of individuals per fishing set) across strata of 1 ° × 1 ° x month. Predictions assumed that (i) the vulnerability of species to bycatch and (ii) the modeled relationships between species-specific bycatch and environmental covariates remained constant across geographic space. To avoid misleading extrapolation to novel environmental conditions, predictions were constrained to the individual ranges of the environmental covariates associated with the observed sets. Monthly predictions were then averaged quarterly. Uncertainty in our model predictions was estimated using maps of coefficients of variation (CVs), which were derived by dividing the standard errors of the GAM coefficients by the mean predictions.

2.3.3. Detection of species-specific bycatch hotspots

We used the 90th percentile of species-specific bycatch predictions (corresponding to the top 10% predicted bycatch values) as the global threshold for identifying bycatch hotspots. For each species and ocean, we calculated the 90th percentile of quarterly bycatch predictions. We then extracted the prediction cells exceeding this threshold and converted them to polygons. Polygons formed by single isolated cells (representing between 1.4 and 8.6% of the hotspots cells in the Atlantic Ocean and between 0.4 and 4.6% in the Indian Ocean) were removed. We then combined species-specific hotspots polygons into a single quarterly map per ocean and smoothed them with a Gaussian kernel using the 'smoothr' package (Strimas-Mackey, 2018). Hotspots corresponding to the 75th percentile of species-specific bycatch predictions were also extracted using the same procedure for comparison.

3. Results

3.1. Models overview

The selected models included 5 to 8 covariates in the AO and 4 to 6 covariates in the IO and resulted in overall lower deviances explained in the IO (mean deviances explained across species: 25% in the AO and 17% in the IO) (Table 1). The most significant environmental covariates across models were DEPTH and SST, while MLD, TKE, and FOBs_DENS were rarely significant. Temporal covariates and random effects were significant in most models. Model goodness-of-fit was satisfying based on residual diagnostics (Figs. C-1 to C-5) and values of PMAE (which were overall lower in the IO) (Table 1).

3.2. Bycatch-environment relationships

Overall, modeled relationships between species-specific bycatch and covariates (compared on the same environmental covariate ranges) were dissimilar between oceans (Fig. 1). Several opposite relationships were found between oceans (e.g., for WAH with SST, DOL with SST, WAH with MLD) and relationships were overall more significant in the AO (e.g., for RRU with MLD, FAL with SST, CNT with CHL). The few comparable relationships between oceans included the relationships of WAH with DEPTH, DOL with SAL, and CNT with MLD. Modeled relationships also appeared dissimilar between species in the same ocean (very few exceptions included the almost identical relationships with DEPTH for FAL and DOL in the AO and the comparable relationships with SAL for all species except CNT in the IO).

3.3. Predictions of bycatch hotspots in the Atlantic Ocean

In the Atlantic Ocean, the prediction envelope excluded the north and south subtropical gyres characterized by deeper mixed layer depth and higher salinity (except for FAL and RRU for which SAL was non-significant) (Fig. 2). The prediction envelope also excluded the Benguela current characterized by lower sea surface temperatures. Bycatch hotspots were predicted throughout tropical and subtropical waters with little overlap between species (Fig. 2, Table 2). FAL hotspots were predicted in the coastal waters of northwestern Africa (year-round) and Gabon and Angola (in quarter 3). FAL hotspots were also predicted in the north and south subtropical gyres (in quarters 1–2 and 4). CNT hotspots were predicted in equatorial waters year-round inside the core area of purse seine fishing. For RRU, WAH and DOL, hotspots were predicted in the coastal waters of Brazil and in offshore waters of the western and central Atlantic (with limited overlap between hotspots). In general, CVs were highest at the northern and southern geographic limits of the prediction envelope (Figs. D-1 to D-5), reflecting the low confidence of relationships with SAL and MLD at the limits of the observed covariate ranges (Fig. 1). Highest CVs were

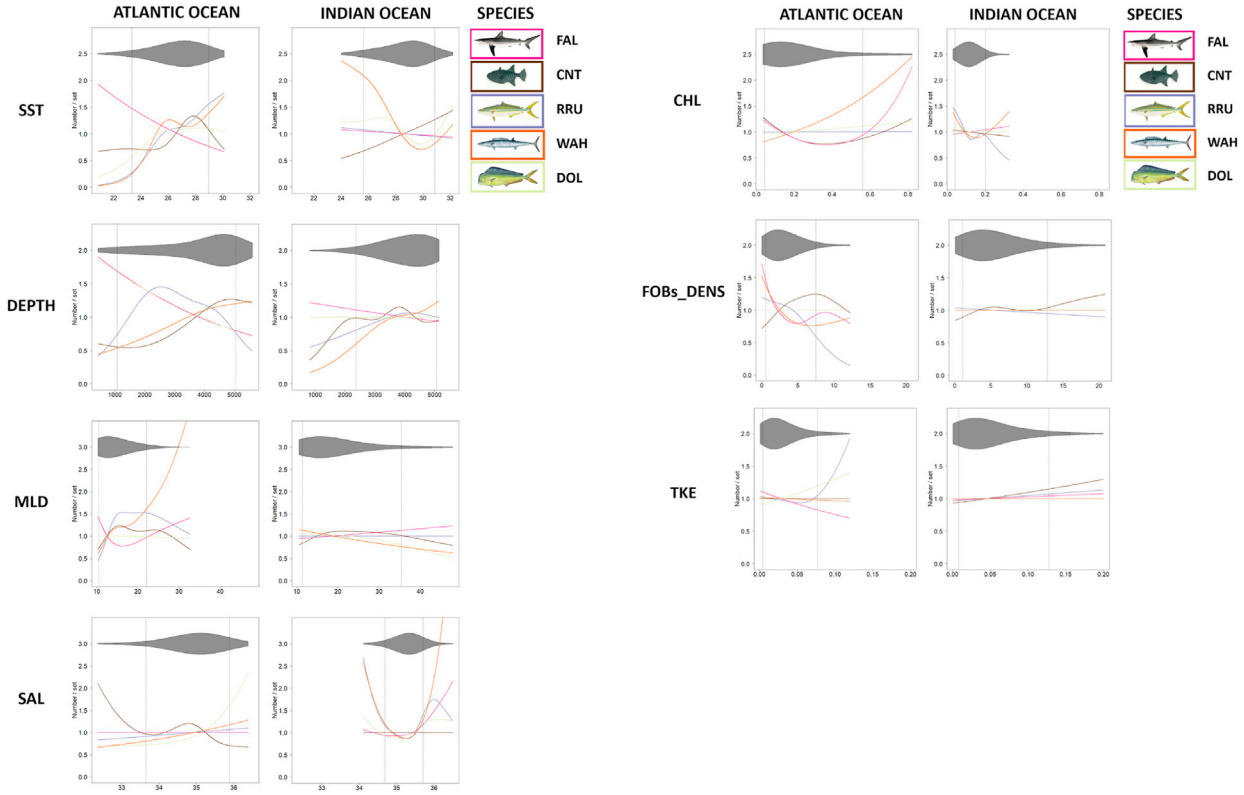

Fig. 1. Statistical relationships between species-specific bycatch (numbers of individuals per FOB fishing set) and environmental covariates. To facilitate comparisons between species and between oceans, plots have the same x and y axes and include relationships with non-significant covariates (dropped from the models). Violin plots show the density of observed sets in covariate space (revealing differing ranges of environmental covariates between oceans). Portions of relationships beyond the 5th and 95th quantiles of the data indicated by vertical dotted lines are associated with lower confidence. We note that relationships are undistinguishable in the Indian Ocean for DOL and WAH with TKE, and for WAH, DOL and FAL shark with FOBs_DENS. Species: FAL: silky shark; CNT: oceanic triggerfish; RRU: rainbow runner; WAH: wahoo; DOL: dolphinfish. Environmental covariates: CHL: chlorophyll-a concentration; SST: sea surface temperature; SAL: surface salinity, MLD: mixed layer depth; TKE: total kinetic energy; FOBs_DENS: floating objects density. Sources for species drawings: https://www.wikipedia.org/, http://www.fao.org, http://www.efishalbum.com.

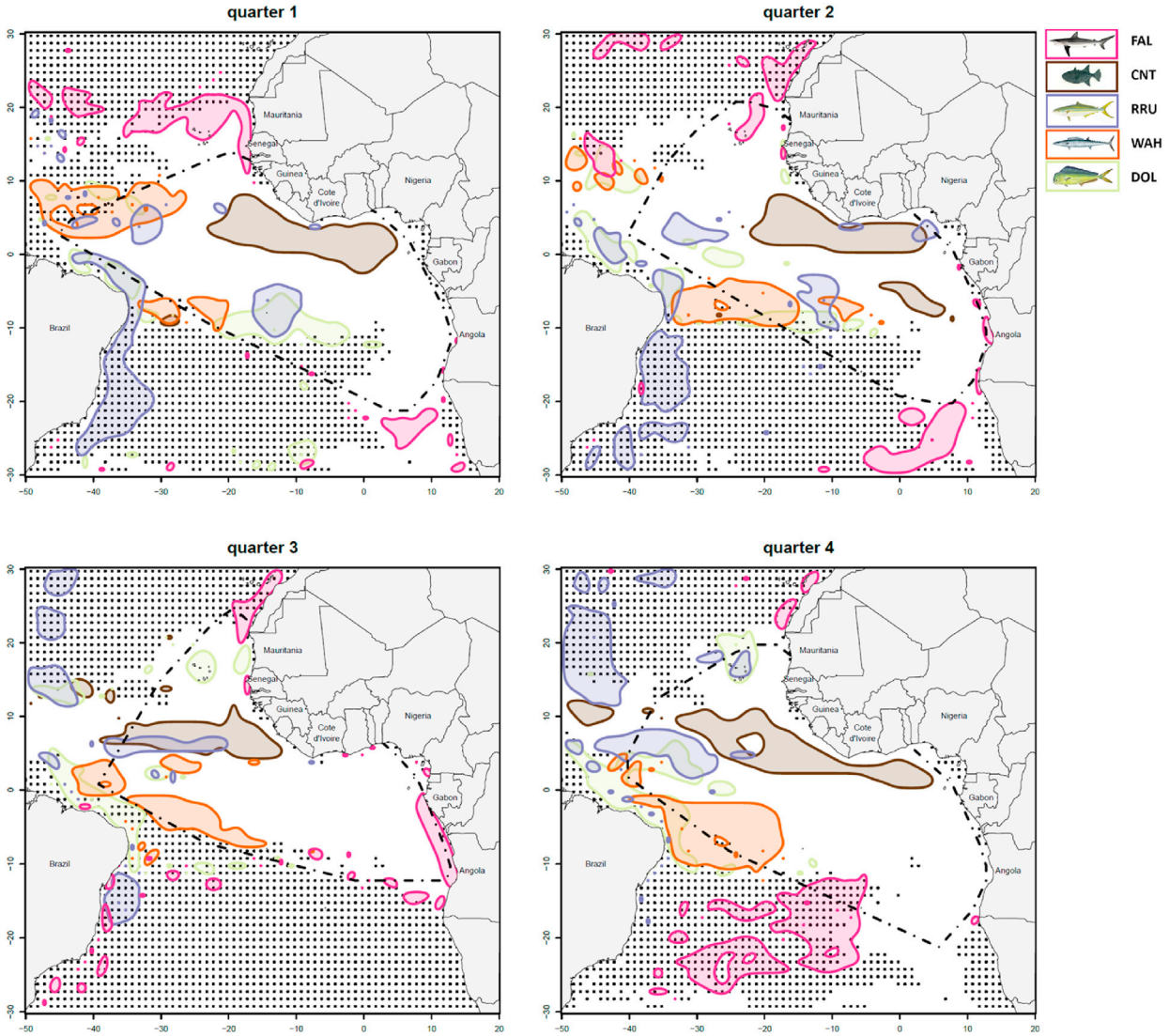

Fig. 2. Predicted bycatch hotspots associated with FOBs for the five species in the Atlantic Ocean, using the 90th percentile of predictions for defining the hotspots. Hotspots were smoothed with a Gaussian kernel. Dashed polygons represent the spatial extents of the tropical purse seine fisheries across all flags derived from the public databases of RMFOs. Black squares delimit areas where predictions would result in misleading extrapolations to novel covariate ranges (except for species for which these covariates were non-significant and therefore dropped for prediction, e.g., salinity for FAL in the AO). Species-specific bycatch predictions and associated CVs are shown in Figs. D-1 to D-5. Maps of bycatch hotspots defined as cells exceeding the 75th percentile of predictions are also provided in Appendix E. Species: FAL: silky shark; CNT: oceanic triggerfish; RRU: rainbow runner; WAH: wahoo; DOL: dolphinfish. Quarters: 1: January–March; 2: April–June; 3: July–September; 4: October–December.

Table 2
90th percentile thresholds used for detecting bycatch hotspots (in numbers of individuals rounded to the nearest unit) across species and oceans.

Species	Ocean	Quarter 1	Quarter 2	Quarter 3	Quarter 4
Silky shark (FAL)	Atlantic	3	5	5	3
	Indian	9	7	10	10
Oceanic triggerfish (CNT)	Atlantic	77	87	112	122
	Indian	126	153	243	172
Rainbow runner (RRU)	Atlantic	155	156	207	137
	Indian	79	67	96	90
Wahoo (WAH)	Atlantic	19	8	15	21
	Indian	7	14	22	14
Dolphinfish (DOL)	Atlantic	6	3	9	10
	Indian	22	20	23	27

associated with FAL and WAH hotspots predicted in offshore waters (ranging from 50 to 80%). In contrast, CVs associated with FAL hotspots in coastal waters and with hotspots of other species were relatively low.

3.4. Predictions of bycatch hotspots in the Indian Ocean

In the Indian Ocean, the prediction envelope excluded the northern Arabian Sea characterized by higher salinity and the Gulf of Bengal and south China Sea characterized by higher chlorophyll-a concentration and lower salinity (except for CNT for which these covariates were non-significant) (Fig. 3). The prediction envelope also excluded colder waters in the southern Indian Ocean (except for FAL and RRU) and deeper waters in the eastern Indian Ocean. Major bycatch hotspots were predicted for four species in the Arabian Sea with strong overlap between species (for FAL, WAH and DOL year-round, and for these three species plus RRU in quarters 2–4) (Fig. 3, Table 2). Other bycatch hotspots were predicted in eastern offshore waters for RRU, WAH and DOL and near the southern geographic prediction limit for these three species and FAL. Contrary to other species, predicted hotspots for CNT were concentrated in offshore equatorial waters year-round. CVs were overall lower than in the Atlantic Ocean but highest (up to 40%) for the predicted hotspots in the Arabian Sea (Figs. D-6 to D-10), reflecting the lowest confidence of relationships with SAL at the upper limits of the observed SAL range (Fig. 1).

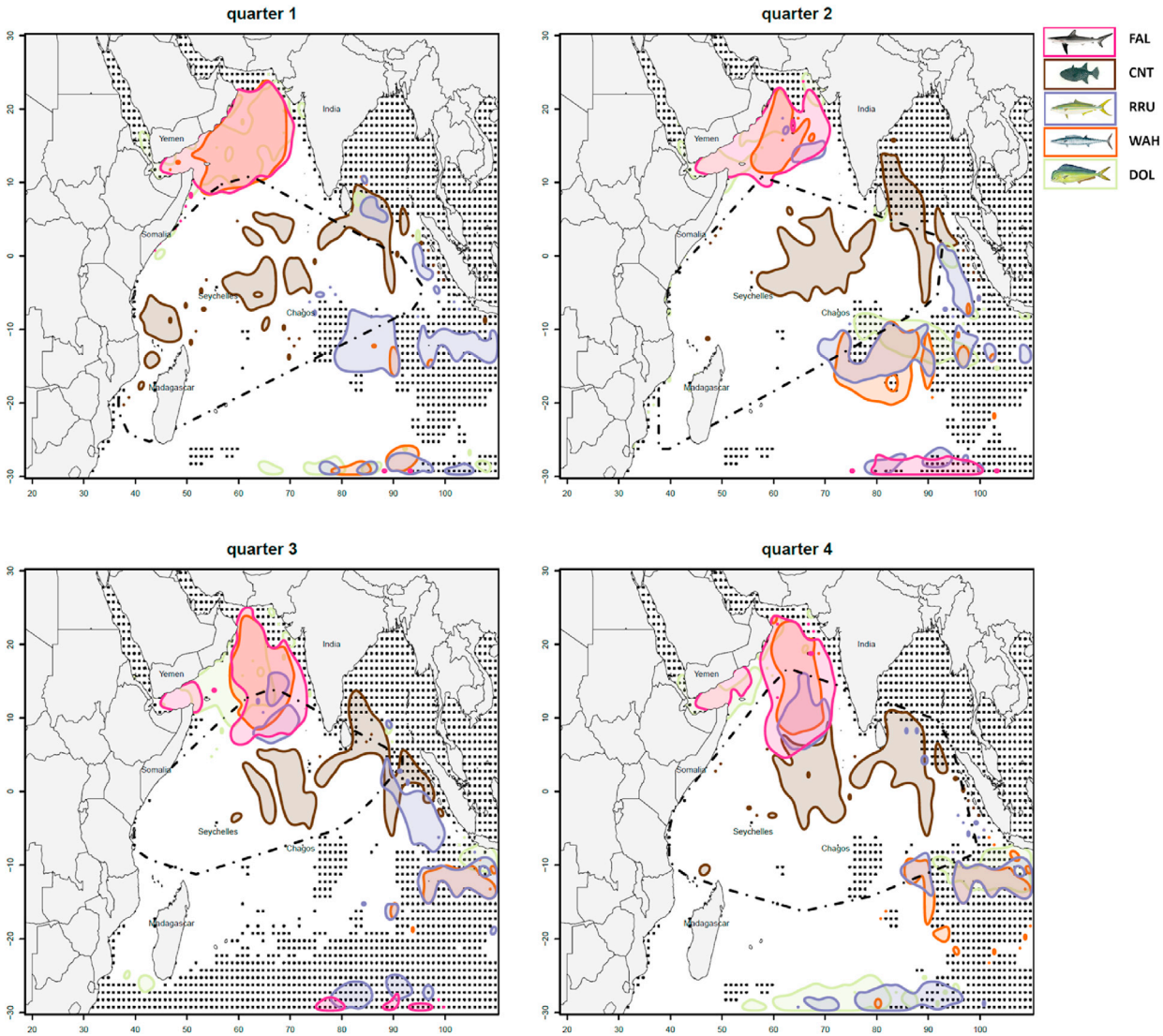

Fig. 3. Predicted bycatch hotspots associated with FOBs for the five species in the Indian Ocean, using the 90th percentile of predictions for defining the hotspots. Same caption as Fig. 2. Species-specific bycatch predictions and associated CVs are shown in Figs. D-6 to D-10. Maps of bycatch hotspots defined as cells exceeding the 75th percentile of predictions are also provided in Appendix E.

4. Discussion

4.1. Applicability for bycatch mitigation

The limited coverage of fisheries observer programs leads to large data gaps in bycatch distribution worldwide, impeding bycatch mitigation across ocean basins. Our habitat modeling approach applied to available fisheries observer programs in TTPSF offers a new way to fill these data gaps. In these fisheries, high bycatch volumes of five dominant species occur at FOBs, raising growing concerns about the impacts of this fishing strategy on pelagic biodiversity (Dagorn et al., 2013b). We combined available fisheries observer programs and environmental data to predict potential species-specific bycatch hotspots associated with FOBs across the tropical Atlantic and Indian oceans.

Even with the lack of evaluation inherent to such extrapolations (discussed in section 4.4), this modeling effort can serve as a first step to assist bycatch mitigation in TTPSF. In the Indian Ocean, the superposition of predicted bycatch hotspots in the Arabian Sea and at the north of the core fishing area for silky shark and three bony fish species suggests that the silky shark may constitute an 'umbrella' species (Roberge and Angelstam, 2004) whose protection would benefit the wider pelagic community. By contrast, the limited overlap of predicted bycatch hotspots in Atlantic waters suggests that species-specific measures would be needed for bycatch mitigation in the Atlantic Ocean. Our predictions also help anticipate bycatch risks associated with possible spatial expansions of TTPSF. For example, they show that expansions off northwestern Africa may lead to the bycatch of silky sharks and that further expansions in the Arabian Sea may result in high volumes of bycatch of four species.

4.2. Ecological interpretation

Our results revealed pronounced differences in bycatch-environment relationships between oceans. These differences probably arose from the use of readily available covariates that represent indirect drivers of resource availability (e.g., CHL and TKE) and have different ecological meaning in different oceanographic regimes (Byrne et al., 2019). There are indeed marked differences in oceanographic regimes of the Atlantic and Indian oceans. For example, productivity is driven by coastal upwelling along west Africa in the AO (Mittelstaedt, 1991), while in the IO, productivity events are driven by an alongshore alignment of summer monsoon winds producing localized upwelling off the coasts of Somalia and the Arabian peninsula (Schott et al., 2009). The use of more direct drivers of resource availability as covariates in HMs would probably result in more consistent species-environment relationships between oceans. Such covariates could be derived from the outputs of ecosystem models such as APECOSM (Maury, 2010), as these model outputs become more accurate at the regional scale.

This study represent the first effort to relate captured individual numbers from fisheries observer programs to the density of floating objects. FOBs form an important component of pelagic ecosystems in tropical oceans (Dagorn et al., 2013a) and their density has importantly increased due to the substantial rise in DFAD deployments in the last decade (Maufroy et al., 2017). In the AO, the estimated inverse relationships between individual numbers and the density of floating objects for some species (e.g., rainbow runner) could indicate higher fragmentation of fish schools above a certain density of objects, as demonstrated theoretically (Sempo et al., 2013). In the IO, weaker relationships for all species could be explained by the larger population sizes in this ocean, potentially leading to more uniform distributions of individuals among FOBs (theoretical work of Sempo et al. (2013)). Future studies should seek to quantify the overall densities of floating objects by combining data from transmitters across all fishing fleets, or ideally, by conducting fishery-independent surveys.

4.3. Habitat modeling assumptions

A central assumption to our habitat modeling approach is the constant vulnerability of species to the fishery across geographic space. When developing HMs from fisheries data, it is important to keep in mind that sampling is conditional on catchability, which reflects both the abundance and the vulnerability of species to the fishing gear (Arreguín-Sánchez, 1996). Catchability is considered a reasonable proxy of species relative abundance when species vulnerability can be assumed constant (Scales et al., 2017). Because our study species nearly exclusively occupy epipelagic waters above the thermocline (Forget et al., 2015; Theisen and Baldwin, 2012; Whitney et al., 2016), it was reasonable to assume they would be consistently vulnerable to the fishery across their distributional ranges.

Another important assumption that underlies all HMs is that individuals sampled through the data occupy suitable habitats for their persistence (Guisan and Thuiller, 2005). An emerging but yet unproven theory proposes that DFADs act as ecological traps potentially driving their associated species to unsuitable habitats with detrimental consequences on their biology (as reflected by their poor body condition) (Hallier and Gaertner, 2008). Using HMs to relate species body condition to environmental covariates (Champion et al., 2020), rather than just abundance, would be helpful for quantifying habitat suitability from a biological standpoint, but at the cost of an important effort in biological sampling across fisheries. Ultimately, fisheries-independent data collected for all species in both oceans would be needed to disentangle the environmental drivers of species abundances. While deployments of pop-up archival transmitting (pSAT) tags have revealed large-scale movements of silky sharks in the IO (Queiroz et al., 2019), such deployments remain challenging on the other four species due their smaller sizes. To date, fisheries observer programs with both high spatio-temporal coverage and high-quality training of observers remain one of the most cost-effective means to learn about the spatial ecology of these species.

4.4. Confidence in extrapolations

In this study, we geographically extrapolated model predictions beyond core purse seine fishing areas within the range of environmental covariates associated with the observed fishing sets. As such, we avoided extrapolations in areas with dissimilar environmental conditions on a-per covariate basis (Mannocci et al., 2015), but not in areas with novel covariates combinations. Approaches excluding novel combinations of covariates, e.g., by delimiting convex hulls in environmental space, would have considerably reduced the geographical extent of extrapolations (Authier et al., 2017). We opted for a less conservative approach that allowed geographical extrapolation over the presumed tropical distributional ranges of our study species (Gaither et al., 2016). The CVs associated with the predictions were highest at the margins of prediction envelopes where environmental covariates values approached their sampled limits. This corresponded in the Atlantic Ocean to the offshore area (spanning hotspots for FAL and WAH), and in the Indian Ocean to the Arabian Sea (spanning hotspots for four species). Both the lowest predicted individual numbers and the lowest densities of sampled covariate values (as shown on the violin plots in Fig. 1) could explain the overall highest CVs in the Atlantic Ocean.

Like in all extrapolation exercises, the quantitative evaluation of predictions is hindered by the lack of species distribution data beyond surveyed regions (Derville et al., 2018; Mannocci et al., 2015; Virgili et al., 2019). Oceanic triggerfish and rainbow runner are principally captured by artisanal fisheries in which reporting is extremely limited (e.g., Pinheiro et al., 2011). Wahoo and dolphinfish are captured by pelagic longlines (Huang and Liu, 2010), but are not subject to mandatory reporting requirements by RFMOs. Silky sharks are caught by pelagic longlines in both the Atlantic Ocean (Coelho et al., 2012; Frédou et al., 2015) and the Indian Ocean (Huang and Liu, 2010) and are subject to mandatory reporting in fishers logbooks (IOTC resolution 15/01 and ICCAT Recommendation 11/08). However, information on shark occurrences remains highly incomplete because of inconsistent reporting by some fleets and uncertain species identification (Fiorellato et al., 2019). Despite this incomplete information, it is worth noting the correspondence between high catches of sharks (all species combined) reported in multiple fisheries in the Arabian Sea and our predicted silky shark hotspots in this region (Fiorellato et al., 2019). Until accurate data can be a collected from fisheries observer programs in these tropical regions, our modeling approach can serve as an initial step to fill the existing gaps.

5. Conclusions

This study offers a novel approach for predicting bycatch hotspots in areas of sparse data by combining fisheries observer and environmental data through habitat models. Our model predictions help address data gaps in the distribution of bycatch in TTPSF, laying a foundation for bycatch mitigation efforts at the basin scale. Our predictions can also serve to anticipate bycatch risks associated with future expansions of these fisheries. This is particularly important as the use of GPS transmitters and echosounders attached to DFADs has already contributed to the expansion of the purse-seine fishing grounds in tropical oceans. Using habitat models to anticipate the potential consequences of such expansions on pelagic communities is critical to move towards an ecosystem approach to fisheries management. Our modeling approach can be more generally applied to derive predictions of bycatch hotspots for other fisheries, species, and data-poor ecosystems.

Declaration of competing interest

The authors declare that they have no known competing financial interests or personal relationships that could have appeared to influence the work reported in this paper.

Acknowledgements

Fisheries observer data collection was funded by the EU DCF program (European Maritime and Fisheries Fun measure 77) and the Orthongel Observateur Commun Unique et Permanent program. LM, FF, and MT were supported by the INNOV-FAD project (European Maritime and Fisheries Fun measure 39). Environmental covariates data used in this study were retrieved from the EU Copernicus Marine Service Information.

Supplementary data

Supplementary data to this article can be found online at https://doi.org/10.1016/j.gecco.2020.e01393.

References

Amandè, M.J., Ariz, J., Chassot, E., de Molina, A.D., Gaertner, D., Murua, H., Pianet, R., Ruiz, J., Chavance, P., 2010. Bycatch of the European purse seine tuna fishery in the Atlantic Ocean for the 2003–2007 period. Aquat. Living Resour. 23, 353–362. https://doi.org/10.1051/alr/2011003.

Arreguín-Sánchez, F., 1996. Catchability: a key parameter for fish stock assessment. Rev. Fish Biol. Fish. 6, 221–242. https://doi.org/10.1007/BF00182344.

Augustin, N.H., Sauleau, E.-A., Wood, S.N., 2012. On quantile quantile plots for generalized linear models. Comput. Stat. Data Anal. 56, 2404–2409.

Authier, M., Saraux, C., Péron, C., 2017. Variable selection and accurate predictions in habitat modelling: a shrinkage approach. Ecography 39. https://doi.org/10.1111/ecog.01633, 001–012.

Byrne, M.E., Vaudo, J.J., Harvey, G.C.M., Johnston, M.W., Wetherbee, B.M., Shivji, M., 2019. Behavioral response of a mobile marine predator to environmental variables differs across ecoregions. Ecography 42, 1569–1578. https://doi.org/10.1111/ecog.04463.

Cameron, A.C., Trivedi, P.K., 1990. Regression-based tests for overdispersion in the Poisson model. J. Econom. 46, 347–364. https://doi.org/10.1016/0304-4076(90)90014-K.

Candy, S.G., 2009. Modelling catch and effort data using generalised linear models, the Tweedie distribution, random vessel effects and random stratum-by-year effects CCAMLR Science, 11: 59–80 (2004). CCAMLR Sci. 16, 221–222.

Cauquil, P., Rabearisoa, N., Sabarros, P.S., Chavance, P., Bach, P., 2015. ObServe: database and operational software for longline and purse seine fishery data IOTC–2015–WPEB11–16. In: Presented at the 11 Th Session of the IOTC Working Party on Ecosystems and Bycatch. Olhão, Portugal.

Champion, C., Hobday, A.J., Pecl, G.T., Tracey, S.R., 2020. Oceanographic habitat suitability is positively correlated with the body condition of a coastal-pelagic fish. n/a Fish. Oceanogr. 29 (1), 100–110. https://doi.org/10.1111/fog.12457.

Coelho, R., Fernandez-Carvalho, J., Lino, P.G., Santos, M.N., 2012. An overview of the hooking mortality of elasmobranchs caught in a swordfish pelagic longline fishery in the Atlantic Ocean. Aquat. Living Resour. 25, 311–319. https://doi.org/10.1051/alr/2012030.

Cortés, E., Arocha, F., Beerkircher, L., Carvalho, F., Domingo, A., Heupel, M., Holtzhausen, H., Santos, M.N., Ribera, M., Simpfendorfer, C., 2010. Ecological risk assessment of pelagic sharks caught in Atlantic pelagic longline fisheries. Aquat. Living Resour. 23, 25–34. https://doi.org/10.1051/alr/2009044.

Dagorn, L., Bez, N., Fauvel, T., Walker, E., 2013a. How much do fish aggregating devices (FADs) modify the floating object environment in the ocean? Fish. Oceanogr. 22, 147–153. https://doi.org/10.1111/fog.12014.

Dagorn, L., Holland, K.N., Restrepo, V., Moreno, G., 2013b. Is it good or bad to fish with FADs? What are the real impacts of the use of drifting FADs on pelagic marine ecosystems? Fish Fish. 14, 391–415. https://doi.org/10.1111/j.1467-2979.2012.00478.x.

Derville, S., Torres, L.G., Iovan, C., Garrigue, C., 2018. Finding the right fit: comparative cetacean distribution models using multiple data sources and statistical approaches. Divers. Distrib. 24, 1657–1673. https://doi.org/10.1111/ddi.12782.

Dunn, P.K., Smyth, G.K., 1996. Randomized quantile residuals. J. Comput. Graph Stat. 5, 236–244. https://doi.org/10.1080/10618600.1996.10474708.

Elith, J., Leathwick, J.R., 2009. Species distribution models: ecological explanation and prediction across space and time. Annu. Rev. Ecol. Evol. Syst. 40, 677–697. https://doi.org/10.1146/annurev.ecolsys.110308.120159.

Fiorellato, F., Geehan, J., Pierre, L., 2019. Review of the Statistical Data Available for Bycatch Species IOTC–2019–WPEB15–07_Rev2.

Fisher, R., Wilson, S.K., Sin, T.M., Lee, A.C., Langlois, T.J., 2018. A simple function for full-subsets multiple regression in ecology with R. Ecol. Evol. 8, 6104–6113. https://doi.org/10.1002/ece3.4134.

Forget, F.G., Capello, M., Filmalter, J.D., Govinden, R., Soria, M., Cowley, P.D., Dagorn, L., 2015. Behaviour and vulnerability of target and non-target species at drifting fish aggregating devices (FADs) in the tropical tuna purse seine fishery determined by acoustic telemetry. Can. J. Fish. Aquat. Sci. 72, 1398–1405. https://doi.org/10.1139/cjfas-2014-0458.

Frédou, L., Tolotti, M.T., Frédou, T., Carvalho, F., Hazin, H., Burgess, G., Coelho, R., Waters, J.D., Travassos, P., Hazin, F.H.V., 2015. Sharks caught by the Brazilian tuna longline fleet: an overview. Rev. Fish Biol. Fish. 25, 365–377. https://doi.org/10.1007/s11160-014-9380-8.

Gaither, M.R., Bowen, B.W., Rocha, L.A., Briggs, J.C., 2016. Fishes that rule the world: circumtropical distributions revisited. Fish Fish. 17, 664–679. https://doi.org/10.1111/faf.12136.

Gilman, E., Chaloupka, M., Read, A., Dalzell, P., Holetschek, J., Curtice, C., 2012. Hawaii longline tuna fishery temporal trends in standardized catch rates and length distributions and effects on pelagic and seamount ecosystems. Aquat. Conserv. Mar. Freshw. Ecosyst. 22, 446–488. https://doi.org/10.1002/aqc.2237.

Gilman, E., Passfield, K., Nakamura, K., 2014. Performance of regional fisheries management organizations: ecosystem-based governance of bycatch and discards. Fish Fish. 15, 327–351. https://doi.org/10.1111/faf.12021.

Guisan, A., Thuiller, W., 2005. Predicting species distribution: offering more than simple habitat models. Ecol. Lett. 8, 993–1009. https://doi.org/10.1111/j.1461-0248.2005.00792.x.

Hallier, J.-P., Gaertner, D., 2008. Drifting fish aggregation devices could act as an ecological trap for tropical tuna species. Mar. Ecol. Prog. Ser. 353, 255–264. https://doi.org/10.3354/meps07180.

Huang, H.-W., Liu, K.-M., 2010. Bycatch and discards by Taiwanese large-scale tuna longline fleets in the Indian Ocean. Fish. Res. 106, 261–270. https://doi.org/10.1016/j.fishres.2010.08.005.

ISSF, 2019. Status of the World Fisheries for Tuna. Oct. 2019. ISSF Technical Report 2019-12.

Kaplan, D.M., Chassot, E., Amandé, J.M., Dueri, S., Demarcq, H., Dagorn, L., Fonteneau, A., 2014. Spatial management of Indian Ocean tropical tuna fisheries: potential and perspectives. ICES J. Mar. Sci. 71, 1728–1749. https://doi.org/10.1093/icesjms/fst233.

Katara, I., Gaertner, D., Marsac, F., Grande, M., Kaplan, D.M., Urtizberea, A., Guery, L., Depetris, M., Duparc, A., Floch, L., Lopez, J., Abascal, F., 2018. Standardisation of Yellowfin Tuna CPUE for the EU Purse Seine Fleet Operating in the Indian Ocean (IOTC No. IOTC–2018–WPTT20–36_Rev).

Kitchell, J.F., Essington, T.E., Boggs, C.H., Schindler, D.E., Walters, C.J., 2002. The role of sharks and longline fisheries in a pelagic ecosystem of the central pacific. Ecosystems 5, 202–216. https://doi.org/10.1007/s10021-001-0065-5.

Kleiber, C., Zeileis, A., 2019. AER: applied Econometrics with R. R package version 1.2-5. https://cran.r-project.org/web/packages/AER/index.html.

Lewison, R.L., Crowder, L.B., Wallace, B.P., Moore, J.E., Cox, T., Zydelis, R., McDonald, S., DiMatteo, A., Dunn, D.C., Kot, C.Y., Bjorkland, R., Kelez, S., Soykan, C., Stewart, K.R., Sims, M., Boustany, A., Read, A.J., Halpin, P., Nichols, W.J., Safina, C., 2014. Global patterns of marine mammal, seabird, and sea turtle bycatch reveal taxa-specific and cumulative megafauna hotspots. Proc. Natl. Acad. Sci. Unit. States Am. 111, 5271–5276. https://doi.org/10.1073/pnas.1318960111.

Lezama-Ochoa, N., Murua, H., Chust, G., Van Loon, E., Ruiz, J., Hall, M., Chavance, P., Delgado De Molina, A., Villarino, E., 2016. Present and future potential habitat distribution of Carcharhinus falciformis and Canthidermis maculata by-catch species in the tropical tuna purse-seine fishery under climate change. Front. Mar. Sci. 3 https://doi.org/10.3389/fmars.2016.00034.

Lopez, J., Alvarez-Berastegui, D., Soto, M., Murua, H., 2020. Using fisheries data to model the oceanic habitats of juvenile silky shark (Carcharhinus falciformis) in the tropical eastern Atlantic Ocean. Biodivers. Conserv. 29, 2377–2397. https://doi.org/10.1007/s10531-020-01979-7.

Mannocci, L., Monestiez, P., Spitz, J., Ridoux, V., 2015. Extrapolating cetacean densities beyond surveyed regions: habitat-based predictions in the circumtropical belt. J. Biogeogr. 42, 1267–1280. https://doi.org/10.1111/jbi.12530.

Maufroy, A., Chassot, E., Joo, R., Kaplan, D.M., 2015. Large-scale examination of spatio-temporal patterns of drifting Fish Aggregating Devices (dFADs) from tropical tuna fisheries of the Indian and Atlantic oceans. PLoS ONE 10. https://doi.org/10.1371/journal.pone.0128023.

Maufroy, A., Kaplan, D.M., Bez, N., De Molina, A.D., Murua, H., Floch, L., Chassot, E., 2017. Massive increase in the use of drifting Fish Aggregating Devices (dFADs) by tropical tuna purse seine fisheries in the Atlantic and Indian oceans. ICES J. Mar. Sci. 74, 215–225. https://doi.org/10.1093/icesjms/fsw175.

Maury, O., 2010. An overview of APECOSM, a spatialized mass balanced "Apex Predators ECOSystem Model" to study physiologically structured tuna population dynamics in their ecosystem. Prog. Oceanogr. 84, 113–117.

Mittelstaedt, E., 1991. The ocean boundary along the northwest African coast: circulation and oceanographic properties at the sea surface. Prog. Oceanogr. 26, 307–355. https://doi.org/10.1016/0079-6611(91)90011-A.

Ortuño Crespo, G., Dunn, D.C., 2017. A review of the impacts of fisheries on open-ocean ecosystems. ICES J. Mar. Sci. 74, 2283–2297. https://doi.org/10.1093/icesjms/fsx084.

Pinheiro, P.B., Hazin, F.H.V., Travassos, P., Oliveira, P.G.V., Carvalho, F., Rêgo, M.G., 2011. The reproductive biology of the rainbow runner, Elagatis bipinnulata (Quoy & Gaimard, 1825) caught in the São Pedro and São Paulo Archipelago. Braz. J. Biol. 71, 99–106. https://doi.org/10.1590/S1519-69842011000100015.

Queiroz, N., Humphries, N.E., Couto, A., Vedor, M., Costa, I. da, Sequeira, A.M.M., Mucientes, G., Santos, A.M., Abascal, F.J., Abercrombie, D.L., Abrantes, K., Acuña-Marrero, D., Afonso, A.S., Afonso, P., Anders, D., Araujo, G., Arauz, R., Bach, P., Barnett, A., Bernal, D., Berumen, M.L., Lion, S.B., Bezerra, N.P.A., Blaison, A.V., Block, B.A., Bond, M.E., Bonfil, R., Bradford, R.W., Braun, C.D., Brooks, E.J., Brooks, A., Brown, J., Bruce, B.D., Byrne, M.E., Campana, S.E.,

Carlisle, A.B., Chapman, D.D., Chapple, T.K., Chisholm, J., Clarke, C.R., Clua, E.G., Cochran, J.E.M., Crochelet, E.C., Dagorn, L., Daly, R., Cortés, D.D., Doyle, T.K., Drew, M., Duffy, C.A.J., Erikson, T., Espinoza, E., Ferreira, L.C., Ferretti, F., Filmalter, J.D., Fischer, G.C., Fitzpatrick, R., Fontes, J., Forget, F., Fowler, M., Francis, M.P., Gallagher, A.J., Gennari, E., Goldsworthy, S.D., Gollock, M.J., Green, J.R., Gustafson, J.A., Guttridge, T.L., Guzman, H.M., Hammerschlag, N., Harman, L., Hazin, F.H.V., Heard, M., Hearn, A.R., Holdsworth, J.C., Holmes, B.J., Howey, L.A., Hoyos, M., Hueter, R.E., Hussey, N.E., Huveneers, C., Irion, D.T., Jacoby, D.M.P., Jewell, O.J.D., Johnson, R., Jordan, L.K.B., Jorgensen, S.J., Joyce, W., Daly, C.A.K., Ketchum, J.T., Klimley, A.P., Kock, A.A., Koen, P., Ladino, F., Lana, F.O., Lea, J.S.E., Llewellyn, F., Lyon, W.S., MacDonnell, A., Macena, B.C.L., Marshall, H., McAllister, J.D., McAuley, R., Meÿer, M.A., Morris, J.J., Nelson, E. R., Papastamatiou, Y.P., Patterson, T.A., Peñaherrera-Palma, C., Pepperell, J.G., Pierce, S.J., Poisson, F., Quintero, L.M., Richardson, A.J., Rogers, P.J., Rohner, C. A., Rowat, D.R.L., Samoilys, M., Semmens, J.M., Sheaves, M., Shillinger, G., Shivji, M., Singh, S., Skomal, G.B., Smale, M.J., Snyders, L.B., Soler, G., Soria, M., Stehfest, K.M., Stevens, J.D., Thorrold, S.R., Tolotti, M.T., Towner, A., Travassos, P., Tyminski, J.P., Vandeperre, F., Vaudo, J.J., Watanabe, Y.Y., Weber, S.B., Wetherbee, B.M., White, T.D., Williams, S., Zárate, P.M., Harcourt, R., Hays, G.C., Meekan, M.G., Thums, M., Irigoien, X., Eguiluz, V.M., Duarte, C.M., Sousa, L.L., Simpson, S.J., Southall, E.J., Sims, D.W., 2019. Global spatial risk assessment of sharks under the footprint of fisheries. Nature 572, 461–466. https://doi.org/10.1038/s41586-019-1444-4.

Redfern, J.V., Moore, T.J., Fiedler, P.C., Vos, A., Brownell, R.L., Forney, K.A., Becker, E.A., Ballance, L.T., 2017. Predicting cetacean distributions in data-poor marine ecosystems. Divers. Distrib. 23, 394–408.

Richards, S.A., 2008. Dealing with overdispersed count data in applied ecology. J. Appl. Ecol. 45, 218–227. https://doi.org/10.1111/j.1365-2664.2007.01377.x.

Roberge, J.-M., Angelstam, P., 2004. Usefulness of the umbrella species concept as a conservation tool. Conserv. Biol. 18, 76–85. https://doi.org/10.1111/j.1523-1739.2004.00450.x.

Roda, M.A.P., Gilman, E., Huntington, T., Kennelly, S.J., Suuronen, P., Chaloupka, M., Medley, P.A., 2019. A Third Assessment of Global Marine Fisheries Discards. Food and Agriculture Organization of the United Nations.

Scales, K.L., Hazen, E.L., Maxwell, S.M., Dewar, H., Kohin, S., Jacox, M.G., Edwards, C.A., Briscoe, D.K., Crowder, L.B., Lewison, R.L., Bograd, S.J., 2017. Fit to predict? Eco-informatics for predicting the catchability of a pelagic fish in near real time. Ecol. Appl. 27, 2313–2329. https://doi.org/10.1002/eap.1610.

Schott, F.A., Xie, S.-P., McCreary, J.P., 2009. Indian Ocean circulation and climate variability. Rev. Geophys. 47, RG1002. https://doi.org/10.1029/2007RG000245.

Sempo, G., Dagorn, L., Robert, M., Deneubourg, J.-L., 2013. Impact of increasing deployment of artificial floating objects on the spatial distribution of social fish species. J. Appl. Ecol. 50, 1081–1092. https://doi.org/10.1111/1365-2664.12140.

Strimas-Mackey, M., 2018. Smoothr: smooth and tidy spatial features. R package version 0.1.1. https://CRAN.R-project.org/package=smoothr.

Theisen, T.C., Baldwin, J.D., 2012. Movements and depth/temperature distribution of the ectothermic Scombrid, Acanthocybium solandri (wahoo), in the western North Atlantic. Mar. Biol. 159, 2249–2258. https://doi.org/10.1007/s00227-012-2010-x.

Virgili, A., Authier, M., Boisseau, O., Cañadas, A., Claridge, D., Cole, T., Corkeron, P., Dorémus, G., David, L., Di-Méglio, N., Dunn, C., Dunn, T.E., García-Barón, I., Laran, S., Lauriano, G., Lewis, M., Louzao, M., Mannocci, L., Martínez-Cedeira, J., Palka, D., Panigada, S., Pettex, E., Roberts, J.J., Ruiz, L., Saavedra, C., Santos, M.B., Canneyt, O.V., Bonales, J.A.V., Monestiez, P., Ridoux, V., 2019. Combining multiple visual surveys to model the habitat of deep-diving cetaceans at the basin scale. Global Ecol. Biogeogr. 28, 300–314. https://doi.org/10.1111/geb.12850.

Whitney, N.M., Taquet, M., Brill, R.W., Girard, C., Schwieterman, G.D., Dagorn, L., Holland, K.N., 2016. Swimming depth of dolphinfish (Coryphaena hippurus) associated and unassociated with fish aggregating devices. Fish. Bull. 114, 426–434. https://doi.org/10.7755/FB.114.4.5.

Wood, S.N., 2019. Mgcv: Mixed GAM Computation Vehicle with Automatic Smoothness Estimation. R Package Version 1.8–27. http://CRAN.R-project.org/package=mgcv.

Wood, S.N., 2017. Generalized Additive Models: an Introduction with R, second ed. CRC Press Book.

Wood, S.N., 2011. Fast stable restricted maximum likelihood and marginal likelihood estimation of semiparametric generalized linear models. J. R. Stat. Soc. Ser. B Stat. Methodol. 73, 3–36. https://doi.org/10.1111/j.1467-9868.2010.00749.x.

Wood, S.N., Augustin, N.H., 2002. GAMs with integrated model selection using penalized regression splines and applications to environmental modelling. Ecol. Model. 157, 157–177. https://doi.org/10.1016/S0304-3800(02)00193-X.

Zuur, A.F., Ieno, E.N., Elphick, C.S., 2010. A protocol for data exploration to avoid common statistical problems. Methods Ecol. Evol. 1, 3–14. https://doi.org/10.1111/j.2041-210X.2009.00001.x.